Journal of the European Ceramic Society 20 (2000) 119–126

Bi(Pb)–Sr–Ca–Cu–O (2223) superconductor prepared by improved sol–gel technique

A. Tampieri[a,*], G. Celotti[a], S. Lesca[a], G. Bezzi[b], T.M.G. La Torretta[b], G. Magnani[b]

[a]*IRTEC-CNR, via Granarolo 64, 48018 Faenza, Italy*
[b]*ENEA-Centro Ricerche Faenza, via Granarolo 62, 48018 Faenza, Italy*

Received 28 January 1999; received in revised form 31 March 1999; accepted 11 May 1999

Abstract

A particular sol–gel process for preparation of BSCCO (2223) powder was devised, settled and tested. Water-in-oil type emulsion technique associated to internal gelation process was chosen, starting from cations' nitrates. Dried powders were calcined for a few minutes at 400°C and then fired at 850°C in steps of 5 h with intermediate grindings: in only 14 h 92% pure (2223) phase was obtained. Powder mean particle size resulted very low (<1 μm) and morphology is characterized by globular grains which are both promising features for subsequent pressure sintering technique. Moreover, the method appears well adaptable to large scale production. © 2000 Elsevier Science Ltd. All rights reserved.

Keywords: Oxide superconductors; Powder-chemical preparation; Sol–gel processes

1. Introduction

Superconducting powder synthesis is still a limiting and conditioning factor in the industrialization process of ceramic superconductors. In this respect wet chemical methods have increasingly been used in the fabrication of high temperature ceramic superconductors[1–4] and if compared to solid-state methods, the chemical routes effectively replace the time-consuming and laborious conventional process, avoiding contamination, loss of stoichiometry and allowing a better control on particle size and morphology.

In particular the sol–gel method is a promising synthetic way for ceramics and recently there have been many attempts to prepare superconducting materials exploiting the advantages the method offers.

The preparative technique described hereafter has been selected as one of the most suitable candidate to avoid the above problems by providing intimate mixing of the metal cations[5–7] on the atomic scale and saving processing time. Water in oil (W/O, wherein aqueous droplets are dispersed in an organic phase) type emulsion technique,[8,9] associated to internal gelation process was used instead of external gelation with ammonia to avoid the formation of ammoniacal complexes and to assure higher homogeneity in shorter time. The small dimensions and different morphology of particles were exploited to prepare highly textured bulk superconductors.

2. Experimental

Bismuth basic nitrate (BDH), lead nitrate (Carlo Erba), strontium nitrate (C.E.), calcium nitrate (C.E.) and copper nitrate (C.E.) in different molar ratio to prepare three nominal stoichiometries: (A) $Bi_{1.9}Pb_{0.35}Sr_2Ca_2Cu_3O_x$, (B) $Bi_{1.7}Pb_{0.3}Sr_{1.8}Ca_{2.3}Cu_{3.1}O_x$ and (C) $Bi_{1.8}Pb_{0.4}Sr_{1.6}Ca_{2.9}Cu_{3.5}O_x$ were dissolved at about 60°C in water containing EDTA as chelant agent. Urea in the ratio metal/urea = 1.4 was added to the previous solution, then the solution was dropped into the vaseline oil (Carlo Erba) containing the emulsifying agent Span 20(BDH) and heated while stirring at 90–120°C.

---

[*] Corresponding author.

PII: S0955-2219(99)00158-2

The volume ratio of vaseline oil and aqueous solution was 3:1 and the addition of emulsifying agent was 0.5–1.0% vol; the blue gel obtained was dried in air at about 200°C following the processes outlined in Fig. 1. Dried gel was calcined at 400°C for 20 min and fired at 855°C for 15–25 h with 2–3 intermediate grindings.

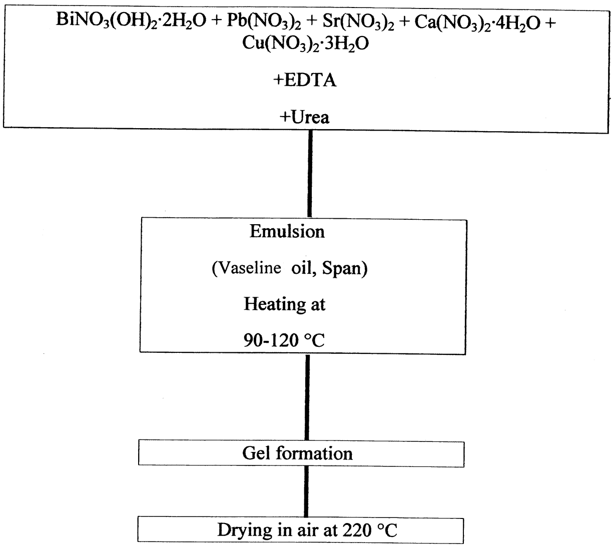

Fig. 1. Outline of the employed sol–gel process.

Transmission FTIR spectra were obtained by Nujol and KBr techniques using a Perkin–Elmer 1600 FTIR spectrometer.

Powder obtained by sol–gel was cold pressed at 700 MPa and pressureless sintered at 855°C for 5 h in air. Afterwards samples were textured by hot-forging using a special apparatus at 840°C under 11 MPa for 80 h.

The density of the samples was measured by Archimedes' method. X-ray diffraction data were taken at room temperature by Rigaku Miniflex diffractometer with CuK_α radiation. The morphology of the powder and dense samples was investigated by means of scanning electron microscopy (Leica Cambridge Ltd) and energy dispersive X-ray spectroscopy (EDS); in the case of powder it was suspended in ethanol and sprayed on the sample holder. Differential and gravimetric thermal analyses were performed on powders with a simultaneous thermal analysis apparatus (Netzsch, STA 409).

Magnetic susceptibility was measured on the powder and dense samples at $H = 0.006$–1 Oe and at a frequency of 333–1000 Hz. Transport properties were measured on dense samples by means of the four probe method using Ag paste contacts, which were dried and hardened at 100°C for 10 min.

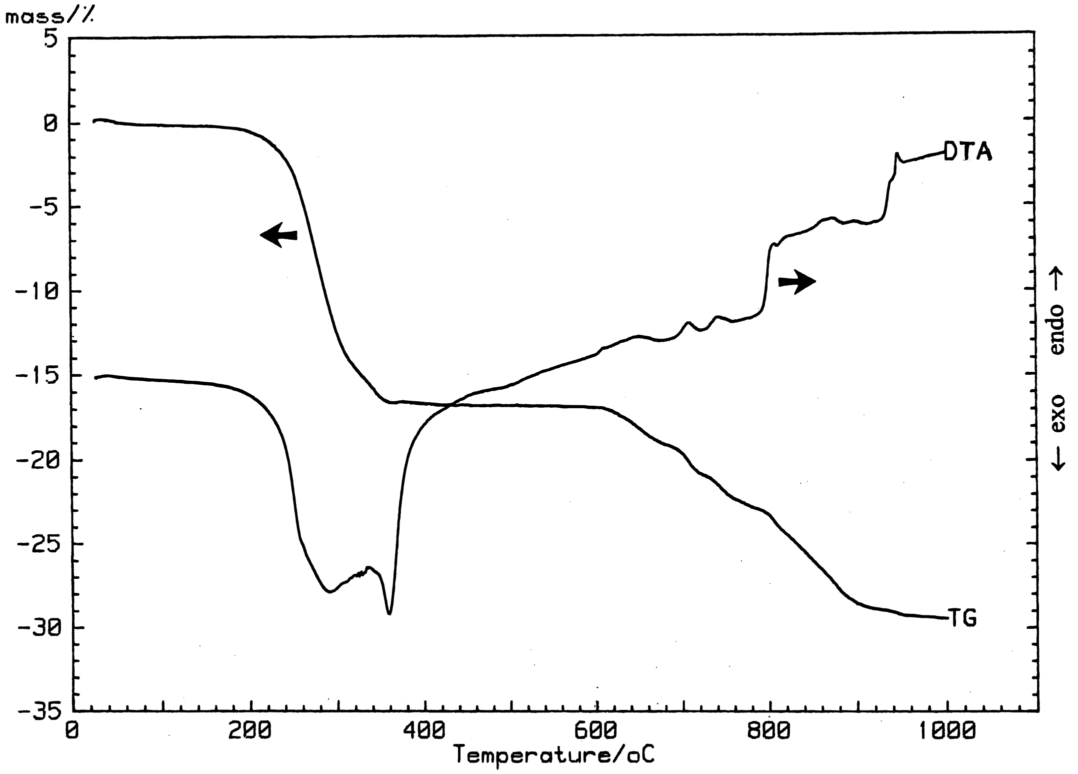

Fig. 2. TG–DTA curves for the gel dried at 200°C.

3. Results and discussion

3.1. Powders

The used method of internal gelation[10] from the emulsioned droplets to the whole mass assures a high homogeneity of the system and the completion of the process in a very short time: this is the most important advantage in respect to external gelation process in which is difficult to assure the complete gelation of the most internal part of the mixture.

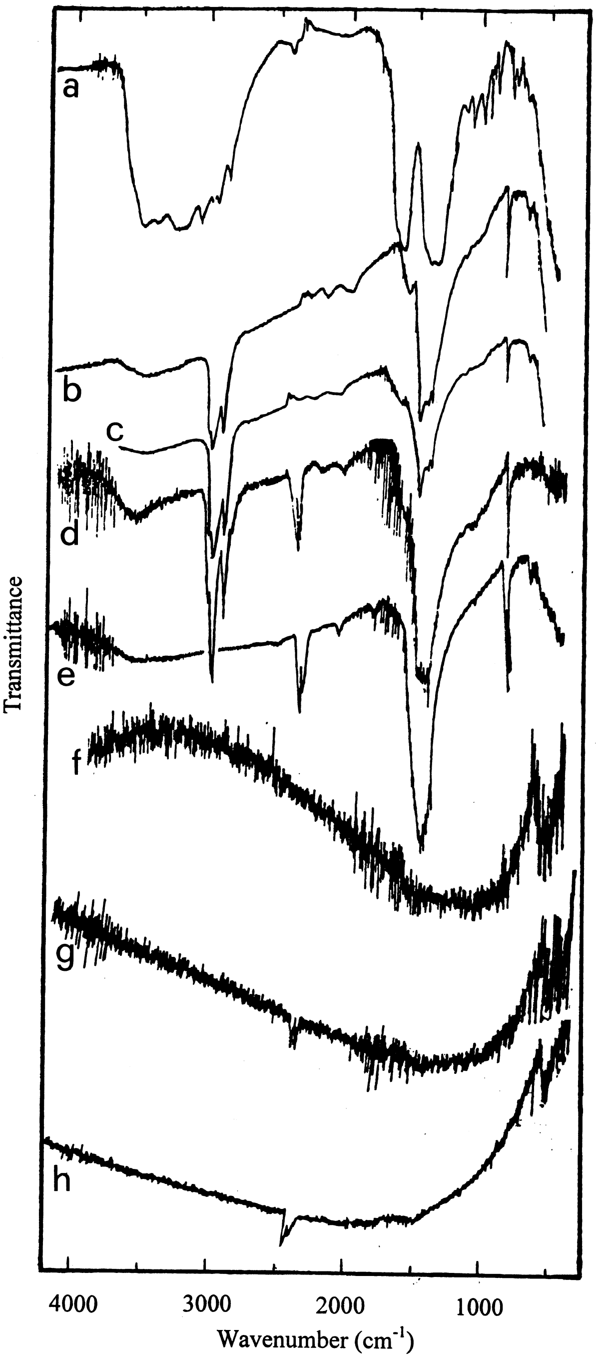

Fig. 3. FTIR spectra obtained at different preparation steps of sol–gel powders: (a) gel as prepared; (b) gel dried at 250°C; (c) gel dried at 300°C (a–c Nujol technique); (d) gel dried at 300°C; (e) gel dried at 350°C; (f) gel fired at 850°C for 5 h; (g) gel fired at 850°C for 10 h; (h) gel fired at 850°C for 20 h (d–h KBr technique).

TG–DTA analysis of the gel dried at 200°C is reported in Fig. 2: the elimination of residual vaseline oil generates a weight loss at $T=160$–310°C, residual acetates would decompose well before 300°C and therefore are hindered by the decomposition of vaseline oil. The DTA peak at 360°C can be attributed to the decomposition of residual nitrates (indeed Ca, Sr, Pb mixed nitrates are detected in the analysed mixture by XRD). The total decomposition of organic fraction is completed at about 500°C followed at $T>600$°C by the carbonates decomposition,[11] which occurs simultaneously with the reaction among oxides.

Thermoanalytical findings are in agreement with the infrared spectra (Fig. 3) obtained at different steps of preparation of the powder: in the gel it is possible to identify several adsorption peaks referred to water (3450 and shoulder at 1640 cm^{-1}), to NH_4^+ group (about 3200 and 3040 cm^{-1}), to acetate group (1590, 1410 and the region 1050–600 cm^{-1}), to nitrate group (about 1370 cm^{-1}) and C–H vibration (2960 and 2920 cm^{-1}) due to Nujol.[12,13]

With the increasing of temperature nitrate group and acetate group peaks tend to disappear and at the same time peaks referred to carbonate group begin to form (1460, 880 and 860 cm^{-1}). In the final spectrum only one peak at about 590 cm^{-1} is observed which can be ascribed to M–O–M bond. From IR spectra it is possible to hypothesize the following evolution from the precursor to the final powder: the presence of acetate group in the precursor gel suggests the formation of compound metal-acetates, originated by starting EDTA-complexes; ammonium group derives from partial decomposition of urea during the water in oil emulsion step. At 250–300°C water and nitrate are still present, but in small amount; decomposition of acetate is going on and decomposition (almost an explosion in the presence of ammonium) of urea is completed: peaks referred to carbonate group (1460 and 880 cm^{-1}) highlight the formation of metal carbonates. At temperature >400°C only peaks (peak at 860 cm^{-1} appears too) due to carbonate are detected (the peak at 2360 cm^{-1}, ascribed to CO_2 depends on the fact that the analysis was performed in air). The spectra of the samples after treatment at 850°C show the evolution of reaction to metal–oxygen–metal bonds.

In Fig. 4 the XRD pattern of the gel dried at $T\approx200$°C is reported in which a complex mixture of amorphous phase and crystalline acetates and nitrates is detected; XRD analysis of the sol–gel precursors with different starting stoichiometries are shown in Figs. 5–7 at different stages of thermal treatment where it can be

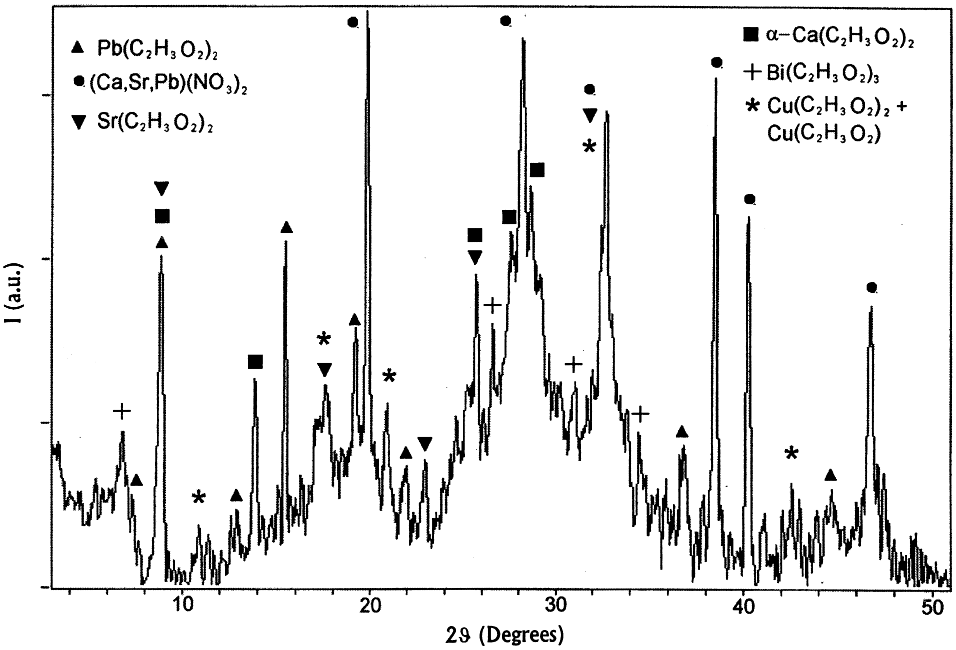

Fig. 4. XRD pattern of gel dried at about 200°C.

seen that the precursor with stoichiometry B exhibits the highest synthesis rate reaching more than 90% of (2223) phase in 14 h of thermal treatment.

SEM analysis (Fig. 8(a)) shows the peculiar morphology of the sol–gel precursor constituted by soft agglomerates of submicronic particles (average size of primary particles ≈200–300 nm) which has to be accounted for as one of the feature responsible of the higher reactivity in respect to the solid state reacted powder (powder S).

To study the reaction path which leads to the formation of (2223) phase, a systematic diffractometric analysis was performed on the mixture isothermally treated at different temperatures in the range 400–850°C for 3 h. The formation of $Bi_6(Ca,Sr)_5O_{14}$ was detected at $T \geqslant 700°C$; as previously reported,[14] this phase plays a crucial role in the superconducting phase formation starting from organic precursor and similarly to what observed in the case of pyrolyzed powder, DTA analysis (performed on the dried gel, using a heating rate of 5°C/min) shows a peak at about 730°C for the formation of $Bi_6Ca_4O_{13}$ and another peak at about 810°C attributed to the transformation of orthorhombic $Bi_6Ca_4O_{13}$ into monoclinic $Bi_6(Ca,Sr)_5O_{14}$. The formation of these intermediates shifts the formation of 2212 phase at higher temperature, so that when (2223) phase starts to nucleate on (2212) particles surface the reaction is accelerated by the higher specific surface; moreover the tendency of (2212) phase to segregate in the core of superconducting particles lowered.

In Fig. 9 the volume fraction of (2223) phase formation in function of synthesis time is reported for sol–gel powders with three different stoichiometries (A, B, C) and compared with powder S: the volume fraction was determined by XRD through the relative intensities ratios of the main peaks (at similar 2θ angles) of (2201), (2212) and (2223) phases, under the hypothesis of comparable scattering powders. The sigmoid shape of the curve relative to the synthesis of powder S is roughly maintained also for sol–gel powders with stoichiometries A and C, where, after an inductive period, an abrupt acceleration can be seen, yielding more than 90% of (2223) phase in 24 and 18 h, respectively. On the other hand, in the case of stoichiometry B, the almost complete absence of the inductive step allows the reaction to be completed in only 14 h. The higher Ca/Sr ratio of powder B in respect to A, is responsible of the higher (2223) formation rate since, as previously reported,[15] Ca plays a crucial role in the first steps of the synthesis; in addition only a limited increase in the Cu content avoids the formation of huge amount of Ca_2CuO_3, which in turn occurs in the case of powder with composition C.

The morphology of the final powder is reported in Fig. 8(b) from wich an average particle size of about 0.5

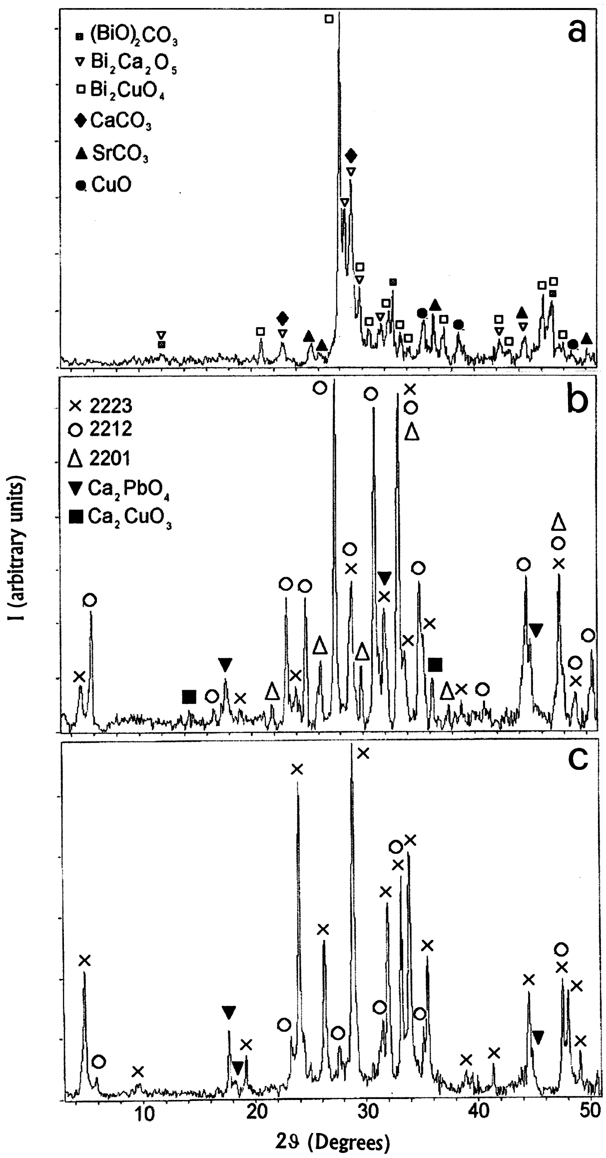

Fig. 5. XRD patterns of gel with stoichiometry A: (a) calcined at 400°C; (b) fired at 850°C for 10 h; (c) fired at 850°C for 25 h.

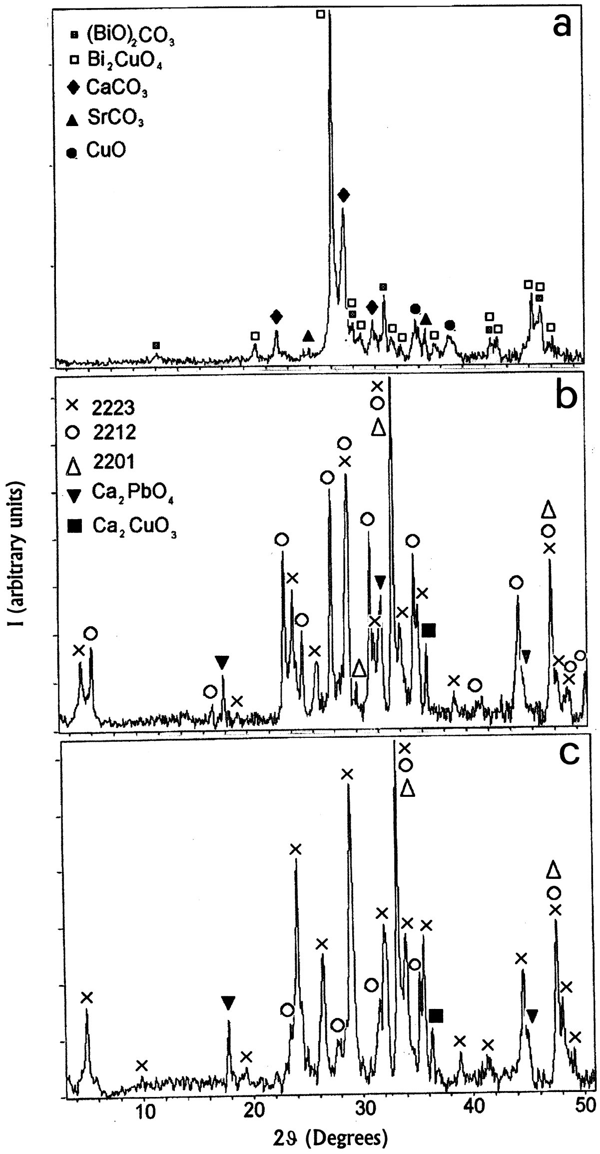

Fig. 6. XRD patterns of gel with stoichiometry B: (a) calcined at 400°C; (b) fired at 850°C for 5 h; (c) fired at 850°C for 14 h.

μm and a nearly isotropic shape can be derived: aspect ratio is ≈2 that is about 10 times lower than that 1 of powder S. Susceptibility measure, performed on the final powder B shows a sharp transition with a diamagnetic onset temperature of 108 K and offset temperature of 104 K.

3.2. Sintered samples

Sintering tests were performed in order to evaluate the workability and stability of the sol–gel powders. Highly textured bulk samples were prepared applying pressure sintering treatments to powders with stoichiometries A and B: the multi-step process including pressureless sintering (850°C/5 h), hot-forging (840°C/80 h) and melt-texturing (885°C/20 min) is described elsewhere.[16] Characteristics of the sintered samples are reported in Table 1.

The use of sol–gel powders allows the attainment of high dense samples characterized by higher orientation factor[17] in respect to those obtained from powder S: indeed the small and isotropic particles of sol–gel powders favour the development of oriented textures

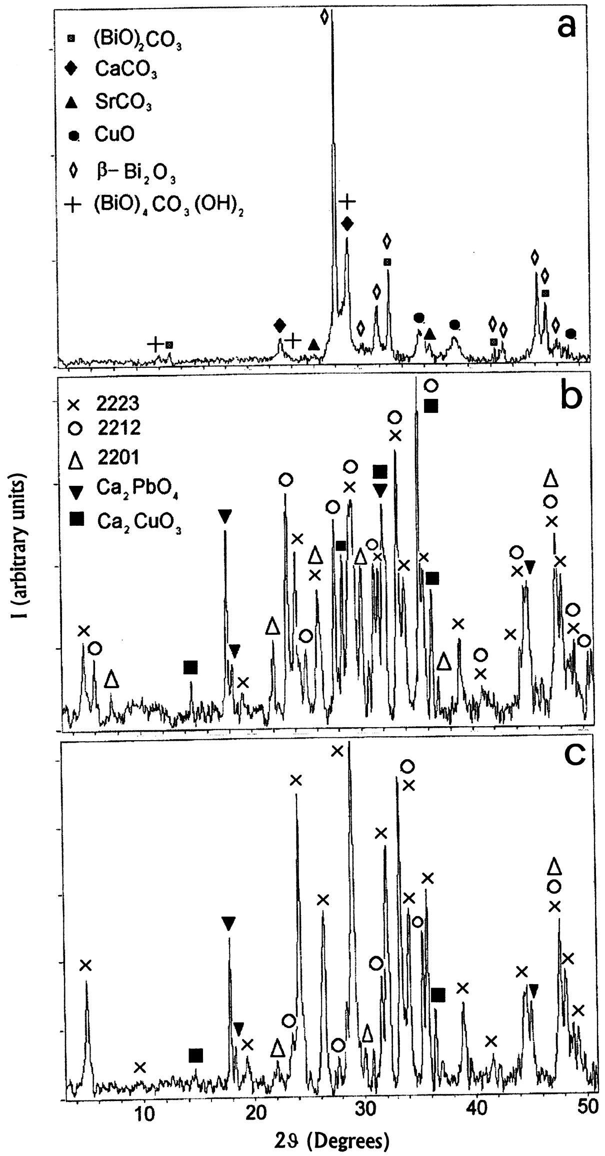

Fig. 7. XRD patterns of gel with stoichiometry C: (a) calcined at 400°C; (b) fired at 850°C for 8 h; (c) fired at 850°C for 18 h.

through their anisotropic growth under the plastic flow action during the pressure sintering process.

During the short high temperature treatment (2223) phase decomposition occurs in sample AI, while in the case of stoichiometry B recrystallization of (2223) phase from liquid is likely to occur[16] and only segregations of non-superconducting phases are detected: in particular dark rounded precipitates, laying among the elongated grains of 2223 phase, were analyzed by X-ray microprobe analysis (EDS) and were found to have a (Ca,Sr)–Cu–O type composition.

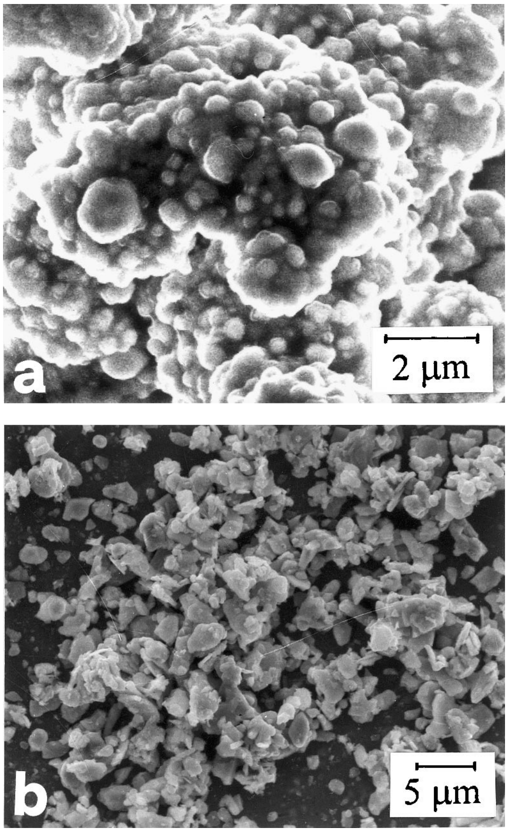

Fig. 8. SEM micrographs showing morphology of sol–gel powders: (a) dried precursor; (b) completely reacted superconducting powder.

It shoud be underlined that sample AI is characterized by low T_{co} value (97 K) and cell parameters slightly enlarged: after restoring treatment in O_2 flux at 400°C for 40 h T_{co} increases up to 103 K. This procedure is not necessary for sample BI in which the above mentioned non-superconducting phases act as intrinsic oxygen reservoir:[16] in fact T_{co} of BI resulted 102 K in the as prepared sample.

In Fig. 10 the susceptibility curves for samples AI and BI are reported in which the biphasic nature of sample AI is evident; on the other hand transport critical current density Jc_t resulted 3000 and 1000 A/cm^2 for sample AI and BI, respectively. It seems interesting to note that the better sample in terms of (2223) phase content and orientation factor is characterized by lower Jc. The higher density of sample AI can be considered as a factor reducing weak links occurrence; in addition the formation of localized precipitates with large dimensions (Fig. 11) seems to affect less transport properties[18] in respect to a similar amount of secondary phases widely distributed in small aggregates. This last feature is a consequence of the

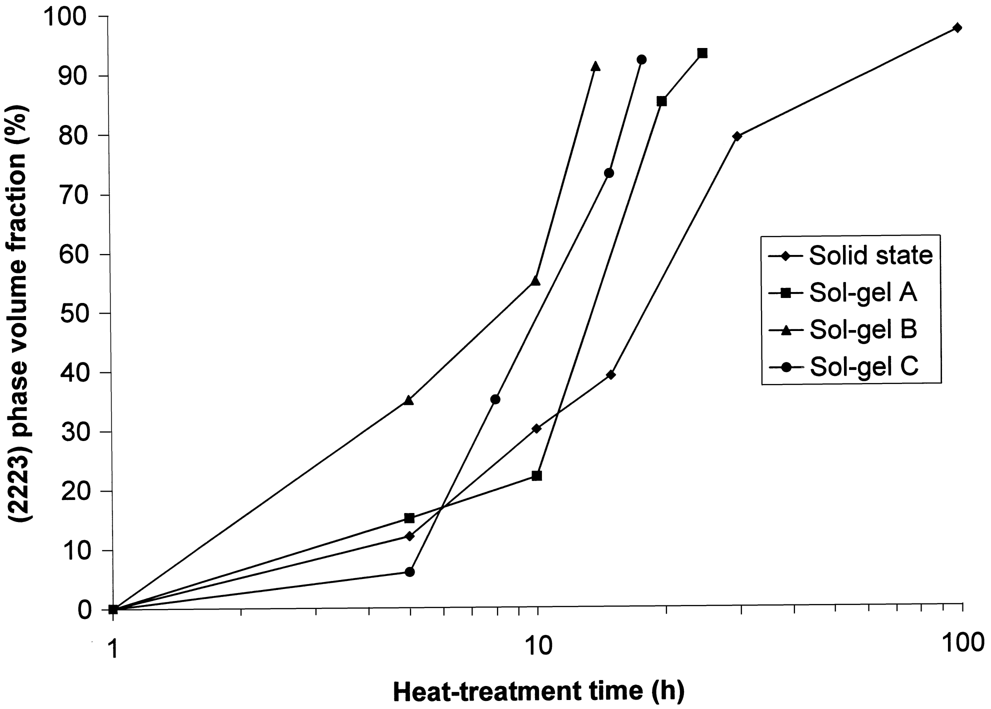

Fig. 9. (2223) volume fraction in ftmction of firing time at 850°C for sol–gel powders with three different stoichiometries and solid state reacted powder.

Table 1
Characteristics of sintered samples using a multi-step process

	2223/2212/2201 (vol%)	R.D. (%)	F (%)	T_{c0} (K)	Jc_t (A/cm^2)
AI	88/10/2	98	78	103[a]	3000
BI	95/3/2	95	80	102	1000

[a] After restoring in O_2.

peculiar behaviour of the sol–gel powder under the described pressure sintering treatment, whose full understanding requires further extensive investigations

4. Conclusions

The preparation of B(Pb)SCCO (2223) by modified sol–gel process provides ≈92% pure phase in only 14 h. The significance of this result is increased by the fact that recent data[2,3,5] still report long synthesis time and low purity, in term of 2223 phase content, for several preparations based on wet methods including sol–gel.

Three different stoichiometries (with Ca/Sr ratios ranging from 1 to 1.8 and Cu molar index from 3 to 3.5) were used in order to study their influence on the synthesis yield and rate in comparison to conventional solid-state method. The transformation reaction from the gel to the final superconducting powder was investigated by IR, TG–DTA and XRD, emphasizing the intermediate compounds decisive for the reaction development.

Sol–gel powder characterized by very small particle size (< 1 μm) and globular shape, turned out to be well suitable for sintering tests: the particles anisotropic growth, during hot-forging, allows the preparation of highly dense and textured samples. During sinter-forging, the high reactivity of sol–gel powder causes a partial decomposition of (2223) phase (being the phenomenon strictly dependent from the powder stoichiometry); the decrease in the superconducting phase content, however, does not cause a correspondent collapse in *Jc* value: these relationships are now under investigation.

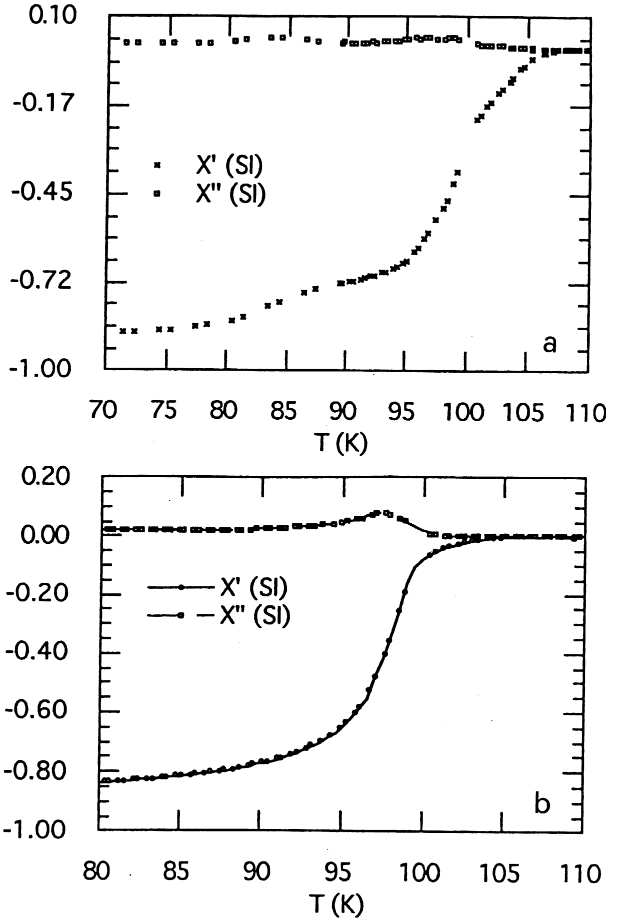

Fig. 10. Magnetic scusceptibility curves for sintered samples: (a) sample AI; (b) sample BI.

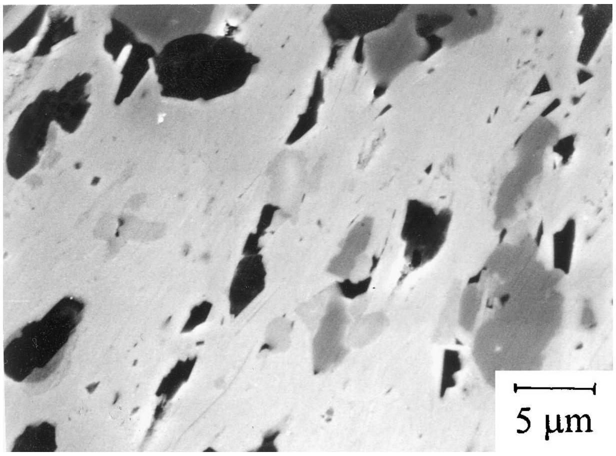

Fig. 11. SEM micrograph of a polished surface of sample AI.

Furthermore the employed method is economically favourable and appears easily expansible to industrial scale production, in contrast with the majority of the so far used techniques.

References

1. Okano, T., Sei, T. and Tsuchiya, T., Preparation of high-Tc superconducting film in the system of Bi–Sr–Ca–Cu–O from sol–gel process and its properties. *J. Mat. Sci.*, 1992, **27**, 4085–4088.
2. Yavuz, M., Maeda, H., Vance, L., Liu, H. K. and Dou, S. X., Effect of ball milling materials and methods on powder processing of Bi2223 superconductors. *Supercond. Sci. Technol.*, 1998, **11**, 1153–1159.
3. Yavuz, M., Maeda, H., Vance, L., Liu, H. K. and Dou, S. X., Powder production methods of Bi–Pb–Sr–Ca–Cu–O superconductors. *Supercond. Sci. Technol.*, 1998, **11**, 1166–1172.
4. Chen, F. H. and Tseng, T. Y., Formation of high-Tc superconducting Bi–Pb–Sr–Ca–Cu oxide films by spray pyrolysis of an oxalate suspension. *J. Am. Ceram. Soc.*, 1990, **73**, 889–892.
5. Sheen, S. R., Chen, D. H., Chang, T. C., Kao, C. H., Huang, J. C., Chou, Y. C., Hsieh, Y. C., Hsieh, Y. H. and Wu, M. K., Rapid formation of the high-Tc phase in (Bi,Pb)–Sr–Ca–Cu–O superconductor via sol–gel method. *J. Mat. Sci.*, 1995, **30**, 1827–1831.
6. Fran, Y. S., Koo, H. S., Chen, F. H., Huang, C. J. and Tseng, Y. T., Synthesis and characterization of Bi–Pb–Sr–Ca–Cu–O superconductor via ethylenediamine chelating. *J. Mat. Sci. Lett.*, 1991, **10**, 58–60.
7. Ruiz, M. T., de la Fuente, G. F., Badia, A., Castro, M., Sotelo, A., Larrea, A., Lera, F., Rillo, C. and Navarro, R., Solution-based synthesis routes to $(Bi_{1-x}Pb_x)_2Sr_2Ca_2Cu_3O_{10+\delta}$. *J. Mat. Res.*, 1993, **8**, 1268–1276.
8. Tampieri, A., Celotti, G., Mammana, E., Bezzi, G., La Torretta, T. M. G. and Magnani, G., Study of the sol–gel processes for BSCCO powders preparation. *Fourth Euroceramics*, 1995, **6**, 445–451.
9. Kook Sun, Y. and Young Lee, W., Preparation of high purity 110 K phase in the Bi(Pb)–Sr–Ca–Cu–O superconductor using the modified citrate process. *Physica C*, 1993, **212**, 37–42.
10. Tanaka, K., Nozue, A. and Kamiya, K., Preparation of Bi,Pb–Sr–Ca–Cu–O superconductor by the sol gel method. *J. Mat. Sci.*, 1990, **25**, 3551–3556.
11. Xu, Q., Bi, L., Peng, D., Meng, G., Zhou, G., Mao, Z., Fan, C. and Zhang, Y., Preparation of high-Tc Bi–Pb–Sr–Ca–Cu–O ceramic superconductor by using the sol gel method. *Supercond. Sci. Technol.*, 1990, **3**, 564–567.
12. Nakamoto, K., *Infrared and Raman Spectra of Inorganic and Coordination Compounds*. Wiley, NewYork, 1986.
13. Kozuka, H., Umeda, T., Jin, J., Miyaji, F. and Sakka, S., Formation of superconducting $YBa_2Cu_3O_y$ through sol–gel method. *J. Ceram. Soc. Jpn.*, 1988, **96**, 350–353.
14. Tampieri, A., Landi, E. and Celotti, G., Mechanisms and kinetics of the synthesis of BSCCO superconducting phases via organometallic precursors. *Physica C*, 1995, **254**, 342–354.
15. Marchetta, M., Dimesso, L., Migliori, A., Masini, R. and Calestani, G., Jc enhancement by partial melting in BSCCO 2223 ceramics. *Il Nuovo Cimento*, 1997, **19D**, 1123–1129.
16. Tampieri, A., Calestani, G., Celotti, G., Masini, R. and Lesca, S., Multi-step process to prepare bulk BSCCO (2223) superconductor with improved transport properties. *Physica C*, 1998, **306**, 21–33.
17. Ma, K. and Pierre, A. C., Grain growth and sintering in Bi–(Pb)–Sr–Ca–Cu–O superconductor made by sol–gel. *J. Mat. Res.*, 1994, **9**, 286–291.
18. Celotti, G., Tampieri, A., Masini, R. and Malpezzi, M. C., Evaluation of structure-related parameters of hot-pressed BISCCO (2223) phase. *Physica C*, 1994, **225**, 346–352.